www.czasopisma.pan.pl PAN POLSKA AKADEMIA NAUK www.journals.pan.pl

Arch. Metall. Mater. **65** (2020), 1, 321-328

DOI: 10.24425/amm.2020.131733

M. LAUBERTOVA[1*], T. HAVLIK[1], L. PARILAK[2], B. DERIN[3], J. TRPCEVSKA[1]

THE EFFECTS OF MICROWAVE-ASSISTED LEACHING ON THE TREATMENT OF ELECTRIC ARC FURNACE DUSTS (EAFD)

In this study, laboratory-scale experiments were carried out to investigate the effects of microwave-assisted alkaline leaching on the treatment of electric arc furnace dusts to recover zinc and lead. Microwave treatment is a new innovative technology in waste treatment and now is an attractive advanced inter-disciplinary field and also environmental friendly. The highest zinc extraction, 50.3% in 60 minutes using 5 M NaOH at 750 W and L:S ratio 20, and lead extraction up to 92.84% was achieved in these same conditions but in 30 minutes. Compared with conventional leaching, the top extraction rate using MW-assisted leaching was higher by 16% (Zn) and 26% (Pb). Zinc presents in the flue dust in the form of franklinite ($ZnFe_2O_4$), its leaching in sodium hydroxide does not occur under the examined conditions, because it is enclosed in a matrix of iron.

Keywords: microwave energy, leaching, industrial waste, EAF dust

1. Introduction

World crude steel production reached 1,691.2 million tonnes (Mt) in 2017, of which the European Union (28) produced 168.7 million tonnes (Mt). About 29% of steel is produced via the electric arc furnace (EAF) route [1]. During EAF steel production, around 20 kg of fine-grained dust (containing Fe, Zn, Cd, Pb, Ca and Cr) per ton of produced steel is generated as a waste [2]. Due to the significant differences between the EAF processes, the contents of zinc, some heavy metals or calcium in the dusts may vary. According to [3] electric arc furnace dusts (EAFD) are classified as hazardous wastes. However, the high contents of zinc (up to 30 wt.%) and iron (up to 49 wt.%) make these dusts very valuable for recycling [4]. Podbrezova Steelworks in Slovakia is an integrated producer of steel and seamless steel tubes. The annual production is 160,000 tonnes of seamless steel tubes, which makes the company one of the leading producers of steel tubes in Europe. In 2017, there was an increase in the production of dust of 5.64% compared to 2015 and an increase of 16.64% compared to 2016 [5]. In principle, eletric arc furnace dusts may be treated using three main groups of methods: pyrometallurgical, hydrometallurgical and combined (pyro-hydrometallurgical). The details of some existing technologies are described elsewhere [6-7]. Each of these has some advantages and some drawbacks. It should be noted that there is still no common and effective technology for the treatment of such wastes. Due to their different mineralogical and chemical compositions, these dusts are treated with different methods. In hydrometallurgical processing, the operation of leaching is essential. The optimum extraction yields of metals without dissolving undesired components can be achieved by appropriate selections of the leaching agent, temperature and pressure. Two types of leaching media are used in EAFD treatment: acidic and alkaline, which may be oxidative and non-oxidative [8-10]. In EAFD, zinc is present in the form of oxide as zincite (ZnO) or franklinite ($ZnFe_2O_4$), which is considerably resistant to leaching [11]. Depending on the leaching medium (i.e. acidic or alkaline), iron either passes into the solution or behaves inertly. Several research efforts have been made to develop a hydrometallurgical method to increase the rate of zinc recovery by utilisation of different leaching media. Different agents can be used for acidic leaching, such as acetic acid or sulphuric acid [9,12-13]. Acidic leaching is more effective than alkaline leaching, but iron passing into the solution causes problems for the subsequent processing of these solutions. Economically, it is appropriate to use sulphuric acid. For practical reasons, it is appropriate to leach at standard temperature and acid concentration values which are sufficient to dissolve the metal of interest. The

[1] INSTITUTE OF RECYCLING TECHNOLOGIES, FACULTY OF MATERIALS, METALLURGY AND RECYCLING, TECHNICAL UNIVERSITY OF KOSICE, LETNA 9, 042 00, KOSICE, SLOVAKIA
[2] RESEARCH AND DEVELOPMENT CENTER OF ZELEZIARNE PODBREZOVA, S.R.O.., KOLKAREN 35, 97681 PODBREZOVA, SLOVAKIA
[3] ISTANBUL TECHNICAL UNIVERSITY, METALLURGICAL AND MATERIALS ENG. DEPT., 34469, ISTANBUL, TURKEY

* Corresponding author: martina.laubertova@tuke.sk

TABLE 1

Summary of studied leaching methods using microwave radiation

Studied material	Type of leaching agent	Temperature [°C]		Maximum extraction of Zn [%]		Leaching time [min]		Source
		*C	**MW	*C	**MW	*C	**MW	
EAFD	NaOH	90	$T_{boiling}$	70	80	30	5	[27]
EAFD	H_2SO_4	—	260	—	92	—	100	[28]
EAFD	NaOH	90	90	74	60.4	240	2	[14]
EAFD	NaOH	—	95	—	85	—	120	[29]
EAFD	H_2SO_4	—	60	—	80	—	90	[30]
EAFD	NaOH	95	—	60	—	15	—	[31]
***BF sludge	H_2SO_4	65	65	87.86	92	7	3	[16]
EAFD	NaOH	95	—	50 80	—	120	—	[32]

* C-conventional leaching; ** MW-microwave leaching; *** Blast Furnace sludge

advantage of acidic leaching is the ability to use more diluted solutions. The disadvantage is that a portion of iron passes into the solution. In alkaline leaching, non-ferrous metals (Zn, Pb) pass into the solution, whilst Fe remains in solid phase in the leaching residue. However, this processing method requires the use of relatively concentrated solutions, which may cause some technical problems. Another disadvantage is the difficult regeneration of such solutions. Zinc in franklinite is difficult to leach, although thermal pre-treatment may overcome this problem [14]. The employment of various leaching techniques has been investigated previously. The advantage of microwave radiation is the transmission of microwaves into the material directly and their subsequent transformation into heat energy. This produces significant reduction inside the material compared to the surface, which may result in a change in the internal structure of the material. Microwave radiation is used as an intensification factor in various technological processes, in particular in the chemical, food and ceramic industries, chemical processes, in mineral processing, wood drying, processing of plastic and glass, vulcanization of rubber, melting metal, processing of coal, microwave assisted extraction, ceramics and waste processing [15], [16-18]. There exist some studies on the microwave leaching of EAFD in the literature [19-24]. Microwave heating efficiency depends on several factors. The most important are: the ability to absorb microwave radiation, microwave frequency, electric power of microwave radiation, and sample weight. Authors [25] investigated the thermal behaviour of EAFD when it was mixed with tetrabromobisphenol (ratio 1:1) under microwave pyrolysis conditions (700°C). In the theoretical part of this paper, attention was paid to the influence of microwave radiation in the process of both acidic and alkaline leaching methods. It shows that leaching combined with microwave radiation may be applied under standard conditions of temperature and pressure, as well as at elevated pressure. The summary of leaching methods using microwave radiation is given in Table 1. This work focuses on the influence of sodium hydroxide concentration on the leaching kinetics of zinc and lead into sodium hydroxide solutions using MW-assisted leaching.

2. Materials and methods

EAFD supplied by Zeleziarne Podbrezova, a. s. (Podbrezova Steelworks, Slovakia) was used for the leaching experiments. The samples were subjected to atomic absorption spectroscopy, the results of which are shown in Table. 2.

TABLE 2

The chemical composition of EAFD

Element	Zn	Fe	Si	Cr	Mn	Pb	Cd	Ca	LOI*
Content [wt%]	17.05	27.23	3.22	0.81	1.03	1.28	0.09	4.42	7.08

* LOI-loss on ignition

The XRD pattern of the EAFD sample is shown in Fig. 1. The mineralogical study showed that metals of interest present in the sample were franklinite $ZnFe_2O_4$, zincite ZnO, magnetite Fe_3O_4, calcite $CaCO_3$, lead monoxide PbO and silica SiO_2.

The granulometric distribution analysis of the EAFD sample was performed using Scanning-photo-sedimentograph, Fritsch GmbH, Analysette. Fig. 2 shows that the measurements result in a size distribution with three maxima: particle diameters of 11 µm, 40 µm and 50 µm. The microstructure, morphology and composition of the dust were also studied using scanning electron microscopy combined with energy dispersive spectroscopy JEOL JMS-35CF with EDX analyzer LINK ANALYTICAL AN10/85S. The morphology of the dust sample is shown in Fig. 3A. The EDS analysis of the observed area shows the presence of Fe, Zn, Ca, Pb, Si, K, S and Cl (Fig. 3B).

A computational thermochemical study was carried out to predict the possible phases in the system depending on the changing parameters. As known, the classical Eh-pH (Pourbaix) diagrams are rather a “predominance diagrams” and they show the regions where various aqueous ions or solid compounds predominate [26]. In this study, a new type aqueous phase diagram by FactSage software was used to distinguish the aqueous species from the solid phases with a real phase boundary. In order

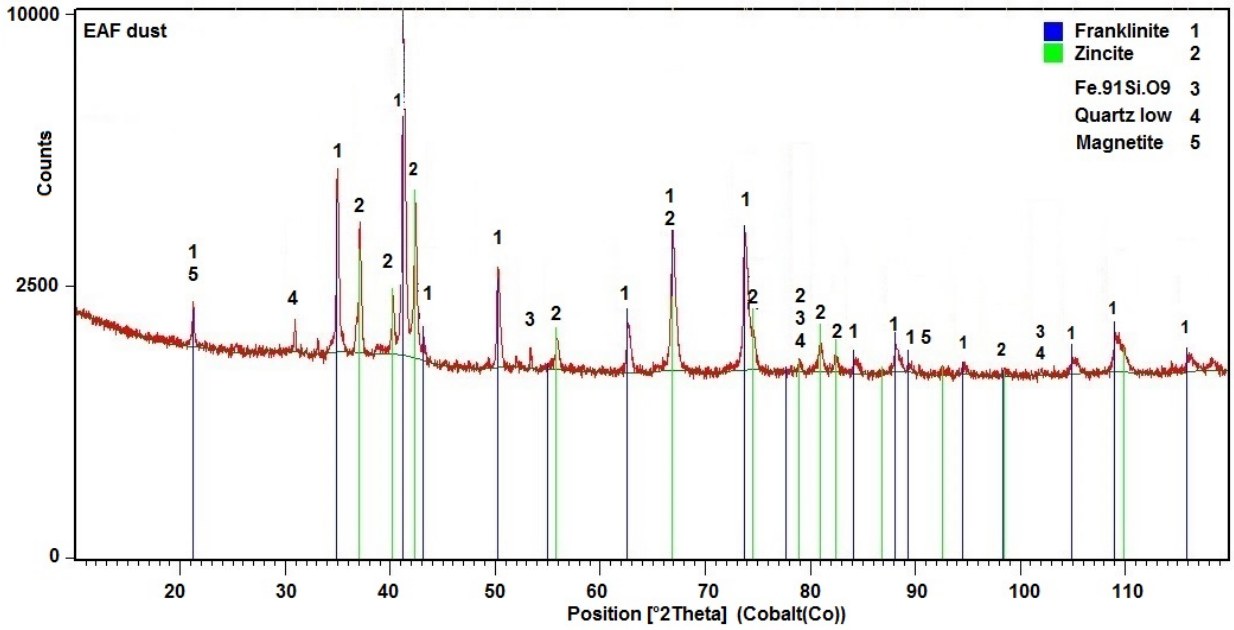

Fig. 1. XRD pattern of the EAFD sample

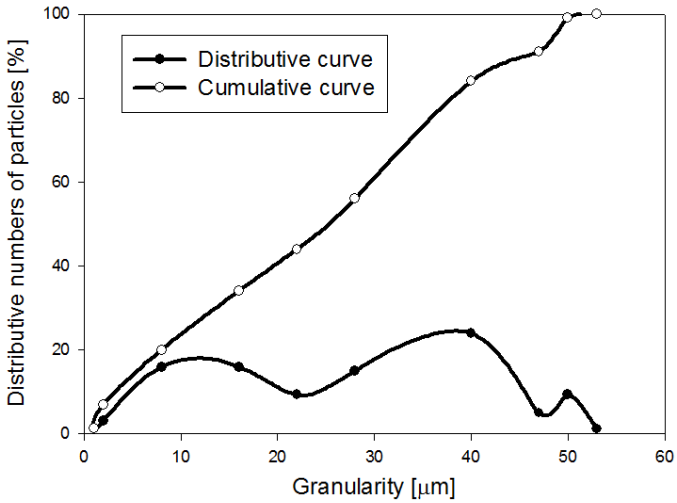

Fig. 2. Granulometric distribution of EAFD sample

to simulate an analogous system, in the calculation, mole values of Fe, Zn, Pb and Ca in one kg of water (mol.kg^{-1}-water) were selected as 0.208, 0.13, 0.0031 and 0.055, respectively. The effect of NaOH (0-8 mol.kg^{-1}-water) on the dissolution behavior of the selected solution was calculated at 104°C. The total pressure of the system was calculated with respect to the reactor temperature (i.e. 104°C) and set to 1.1555 atm. The aqueous phase diagram of H_2O-NaOH-Fe-Zn-Pb-Ca system calculated with the FactSage-Phase Diagram module is shown in Figure 4. The y-axis is the oxidation potential, log pO_2, which is related to Eh, whereas x-axis is the NaOH concentration as mol/kg H_2O in the solution. As seen in the figure, pH level is high even at low concentrations of NaOH. Pb becomes soluble after the pH level of the solution is beyond 11.5, whereas $Ca(OH)_2$ is stable throughout the whole region. The free ZnO in the solution dissolves completely after around 3 kg.mol^{-1} of NaOH. However,

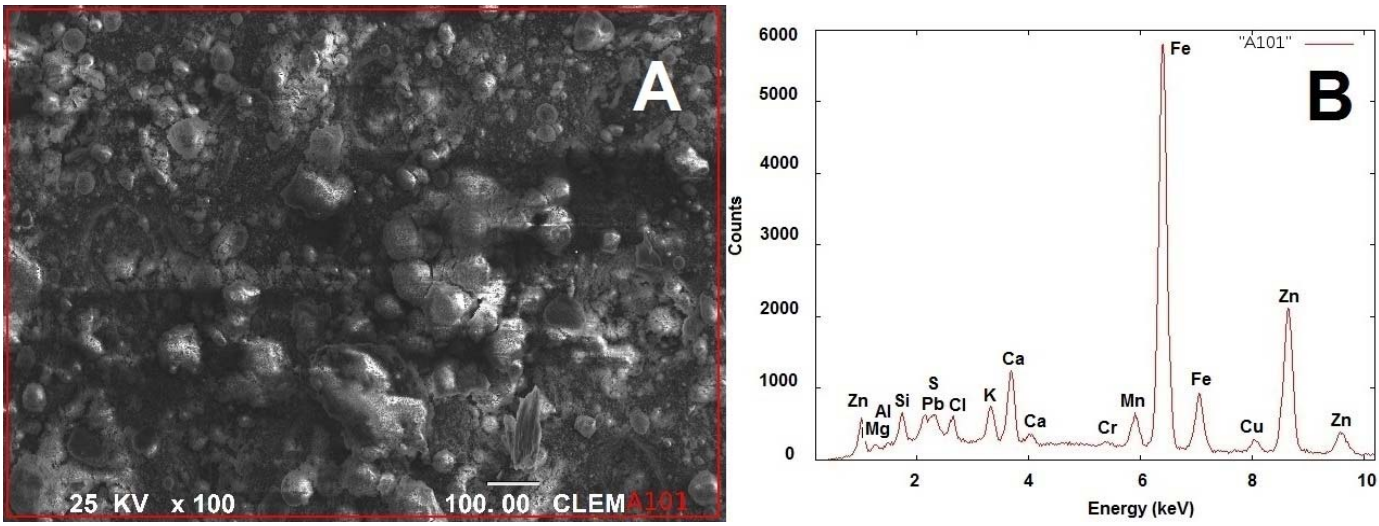

Fig. 3. (A) SEM image of EAFD sample, (B) EDS analysis of EAFD sample

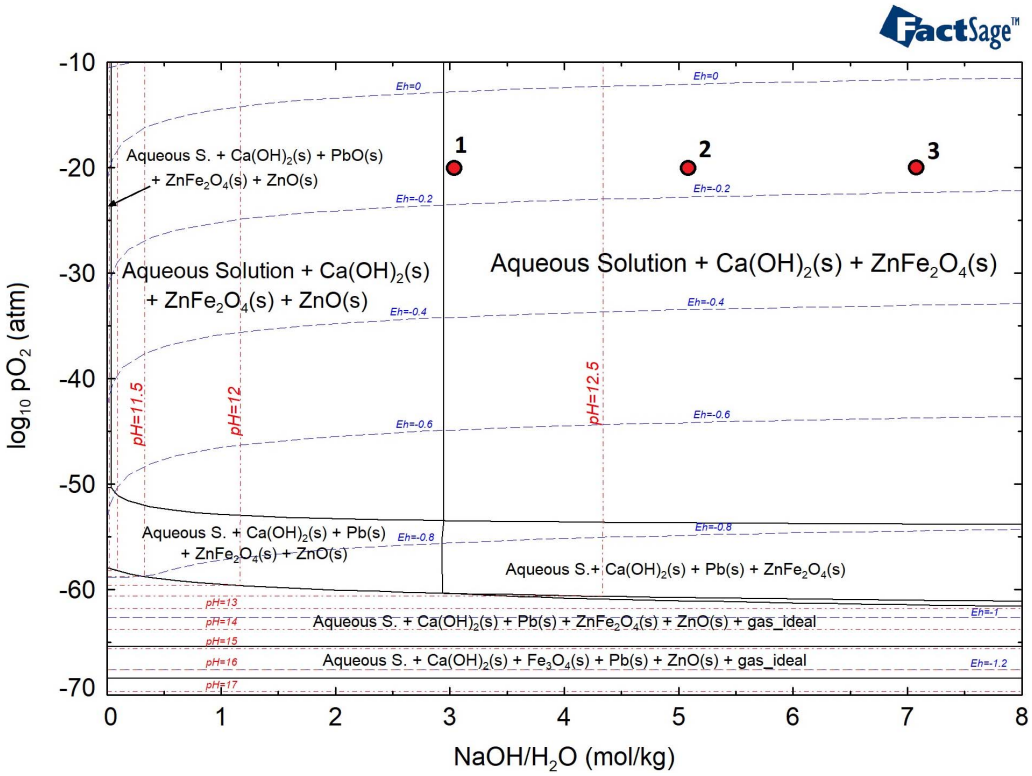

Fig. 4. An aqueous phase diagram with calculated partial O_2 pressure vs. NaOH molality for the system H_2O-NaOH-Fe-Zn-Pb-Ca which is designed for the present experimental conditions

the calculations results showed that a complete dissolution of $ZnFe_2O_4$ is not achievable at any leaching conditions. The compositions and amounts of the aqueous phase and solids that present in the system can be also calculated with FactSage - phase diagram module for the designated locations [26]. For example, at fixed oxidation potential, log pO_2 = –20 (atm), the amounts of the solid $ZnFe_2O_4$ from point 1 through 3, were calculated as 0.001738 mol (pH = 12.365), 0.001705 mol (pH = 12.551) and 0.00165 moles (pH = 12.671) in one kg of water, respectively. It can be concluded that even high amounts of NaOH hardly influence the dissolution behavior of $ZnFe_2O_4$ at 104°C.

In our experimental studies, MW-assisted and conventional leaching of EAFD were carried out in NaOH alkaline leaching medium at concentrations of 1; 2; 3; 4; 5 and 6 M. For comparison, the conventional leaching experiments were done under the same conditions. The dissolution rates of zinc and lead during the leaching processes and the morphologies of solid residues were investigated. The schematic representation of the experimental set-up is shown in Fig. 5. It comprises a leaching plastic reactor closed with a plug (3), with a cooler (5) and a pipette (4) to collect the liquid sample, which are inserted into the reactor. The reactor was placed in a selfmodified microwave cavity with an adjustable output in the power range of 90-900 W at a frequency of 2.45 GHz. Microwave energy was emitted from the magnetron (2). The temperature of the reactor was measured with a manual non-contact thermometer (Raytek Raynger MX4).

Since the particles of EAFD are fine, no sieving was performed on the samples before leaching. The procedure of the

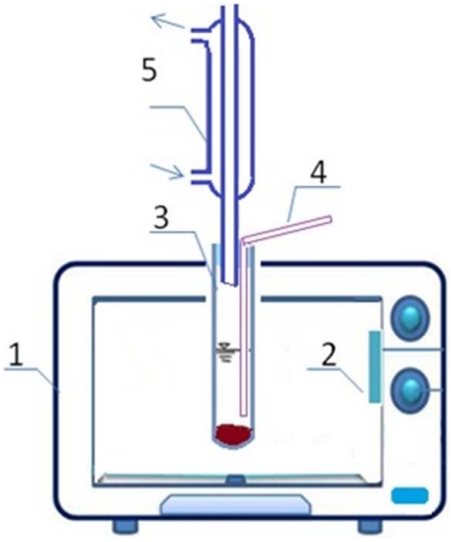

Fig. 5. Schematic diagram of the MW-assisted leaching system. 1 – microwave cavity, 2 – magnetron, 3 – leaching reactor, 4 – pipette, 5 – cooler

experiment was as follows: 200 ml of NaOH solution was poured into the reactor and the output of 750 W was set. After bringing to the boil, after approx. 2 minutes, 10 g of sample was added and leaching time was set at 60 minutes. The weight of 10 grams of dust and the volume of 200 ml of leaching agent produced a liquid to solid phase ratio L:S 20. At lower concentrations of NaOH solution, the entire course of leaching was accompanied by a rapid boil and intense stirring of the pulp. When the solution concentration was higher than 4 M, the boil was quiet, which may

be due to the higher density of the pulp. Samples were taken in the 1st, 5th, 10th, 15th, 30th and 60th minute. The temperature of the reactor was measured as 104°C throughout all experiments. In a microwave heated reactor, the average temperature of the solvent can be at a significantly higher temperature than the atmospheric boiling point (+5°C). After the present time elapsed and the mixture cooled down, it was filtered and the volume of the solution after leaching was measured. The samples were subjected to chemical analysis using the AAS method, which confirmed that no iron passed into the solution during alkaline leaching, or only in a slight amount. For comparison, experiments using conventional leaching of EAFD at 95°C, L:S=20 were also carried out, and samples were taken at the same time intervals as for MW-assisted leaching. The experiments involving conventional leaching made use of the apparatus [9] consisting of a plastic reactor placed in a water bath. With a thermostat, it was possible to maintain a constant temperature throughout the process of leaching. Mechanical agitation of the leaching medium was performed with a plastic agitator, the speed was set to 300 rpm, the pH of the solution was 13-14. An X-PANalytical X´Pert PRO MRD (Co-Kα) X-ray diffractometer was used for qualitative phase analysis of solid residues from the leaching process, and then they were inspected with a Dino-Lite ProAM413T optical microscope. SEM/EDX analysis was performed on the JEOL JSM 35 CF, EDX: LINK AN 10/85S device.

3. Results and discussion

3.1. The effect of sodium hydroxide concentrations

Figs. 6 (A) and (B) show the effect of leaching time on the zinc and lead recovery rates, with sodium hydroxide concentrations in the range of 1-6 M and liquid to solid ratio L:S 20 using MW-assisted leaching.

In both cases, at low concentrations of NaOH leaching agent only small amounts of zinc (2-9%) passed into the solution. With increasing concentration of the leaching agent, the amount of zinc passing into the solution increased smoothly. When microwave energy was applied, after 60 minutes of leaching there was higher extraction of zinc into the solution (48.72%). However, up to the 5th minute there was higher partial extraction of zinc with conventional leaching (19.52-27.46%) than with MW-assisted leaching (4.28-7.22%). This is because during conventional leaching the pulp was stirred from the very beginning using an agitator. During MW-assisted leaching, the pulp was stirred using only the boiling of the liquid itself. Such stirring of the pulp was insufficient due to the high density of leaching solution, i.e. 6 M NaOH, and therefore the pulp was stirred insufficiently. Figs. 7 (A) and (B) show the effect of leaching time on the zinc and lead recovery rates with sodium hydroxide concentrations in the range of 1-6 M and liquid to solid ratio L:S 20 using conventional (C) leaching.

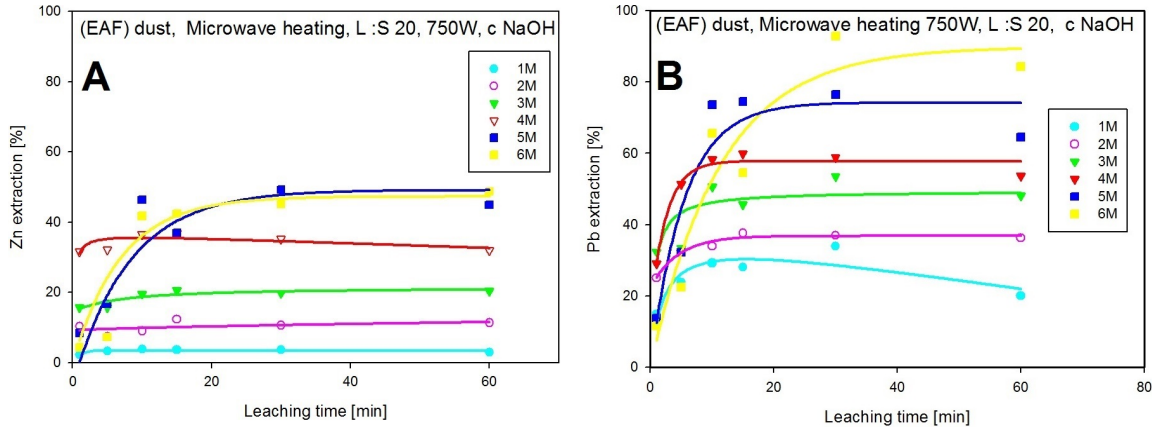

Fig. 6. Effects of time and NaOH concentration on (A) Zn and (B) Pb extraction with MW-assisted leaching

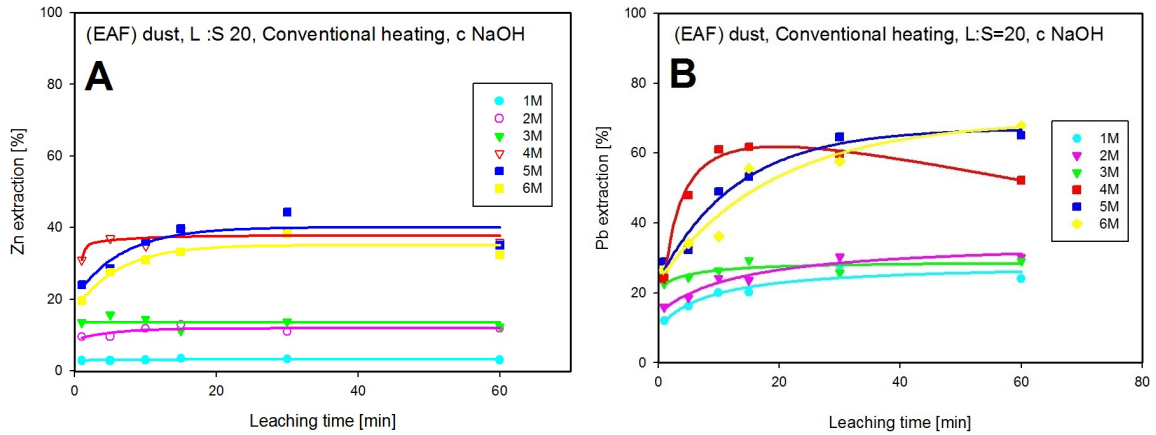

Fig. 7. Effects of time and NaOH concentration on (A) Zn and (B) Pb extraction with conventional leaching

3.2. The comparison of MW-assisted leaching and conventional leaching

Figs. 8 (A) and (B) show the comparison of MW-assisted and conventional leaching on the zinc and lead recovery rates with L:S = 20 and 6 M NaOH solution. The highest lead extraction (92.84%) was reached after 30 minutes of MW-assisted leaching, but in the final minutes the extraction decreased to 84.26%. Again, up to the 5th minute there was higher partial extraction of lead with conventional leaching (26.47-34.25%) than with microwave leaching (11.54-22.45%). The highest lead extraction in conventional NaOH leaching was 67.79%. Compared with conventional leaching, the top extraction rate using MW-assisted leaching was higher by 16% (Zn) and 26% (Pb). These experiments were carried out under comparable conditions.

3.3. The characteristic of the solid residue

Fig. 9 represents the XRD results for the EAFD sample and the residues of the conventionally-leached products at different NaOH concentrations after 60 min. The results show that whereas zincite tends to diminish with increasing NaOH concentration, franklinite remains intact. Similarly, even though zincite dissolves easily in the MW-assisted leaching process, franklinite remains unreacted (Fig. 9B). Xia and Pickles [27] proved decomposition of a part of zinc ferrites by 5-10% increased recovery of Zn in solution by MW assisted leaching, but this argument, however, was not supported by any evidence. The result of the XRD analysis of the leach residue from this research, generated in 6M NaOH at a temperature 104°C using MW-assisted leaching indicated that all zinc ferrite dissolution does not occur, under examined leaching conditions. This statement is based on (Fig. 9B).

SEM images of the EAFD sample and residue particles after MW-assisted leaching and conventional leaching with 6 M NaOH and 60 minutes of leaching are presented in Fig. 10(A-C). Fig. 11(A) shows the globular shape of dust particles before leaching. The larger particles are coated with very fine particles. Very similar rounded particles are also present in Figs. 10(A) and (C). The results of EDS analysis of these particles given in Figs. 11(B1) and (C1) confirm the existence of franklinite in both leached products under the given conditions. The absence of lead in both residues is due to its high dissolution rate during leaching. The EDS analysis also shows the presence of Ca, which remains in the solid residue in the form of $Ca(OH)_2$.

4. Conclusions

The aim of the experimental part of this work was to study the leaching behaviors of Zn and Pb in EAFD under alkaline conditions with the aid of microwave radiation, as well as to observe the behavior of Zn in franklinite. The research results can be summarized as follows:

1) Alkaline leaching of EAFD is selective; iron does not pass into NaOH solution, but remains in the solid residue and behaves inertly in both conventional and MW-assisted leaching. This fact may seem like an advantage for the extraction of zinc. Another advantage is the fact that, during leaching using microwave radiation, the input material – EAFD- does not require previous mechanical pre-treatment.
2) The experimental results also confirm the fact that with increasing concentration of NaOH, the extraction of Zn and Pb into the solution increases. MW-assisted leaching tended to increase the extraction of interest metals by 17%. In MW-assisted leaching Pb extraction of 93% was already achieved in the 30th minute compared to conventional leaching where, under the same conditions, extraction of 67.7% was achieved in the 60th minute.
3) From the results of X-ray and SEM/EDX analyses it can be concluded that, under the given conditions, zinc was leached only from zincite using both leaching methods. Zinc present in the dust in the form of franklinite did not pass into the solution during leaching, which is why lower extraction of the said metal was achieved.

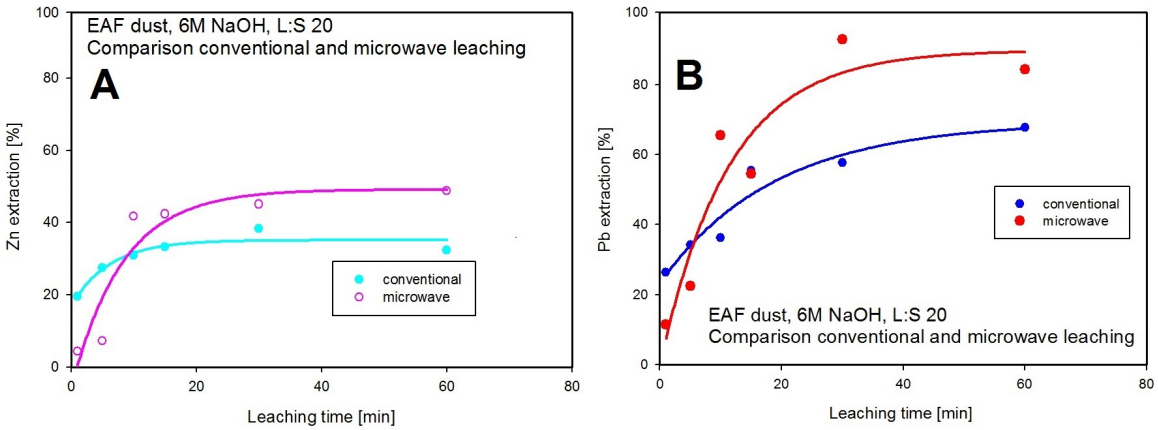

Fig. 8. Comparison of MW-assisted and conventional leaching on (A) Zn and (B) Pb recovery rates with L:S=20 and sodium hydroxide concentration of 6 M

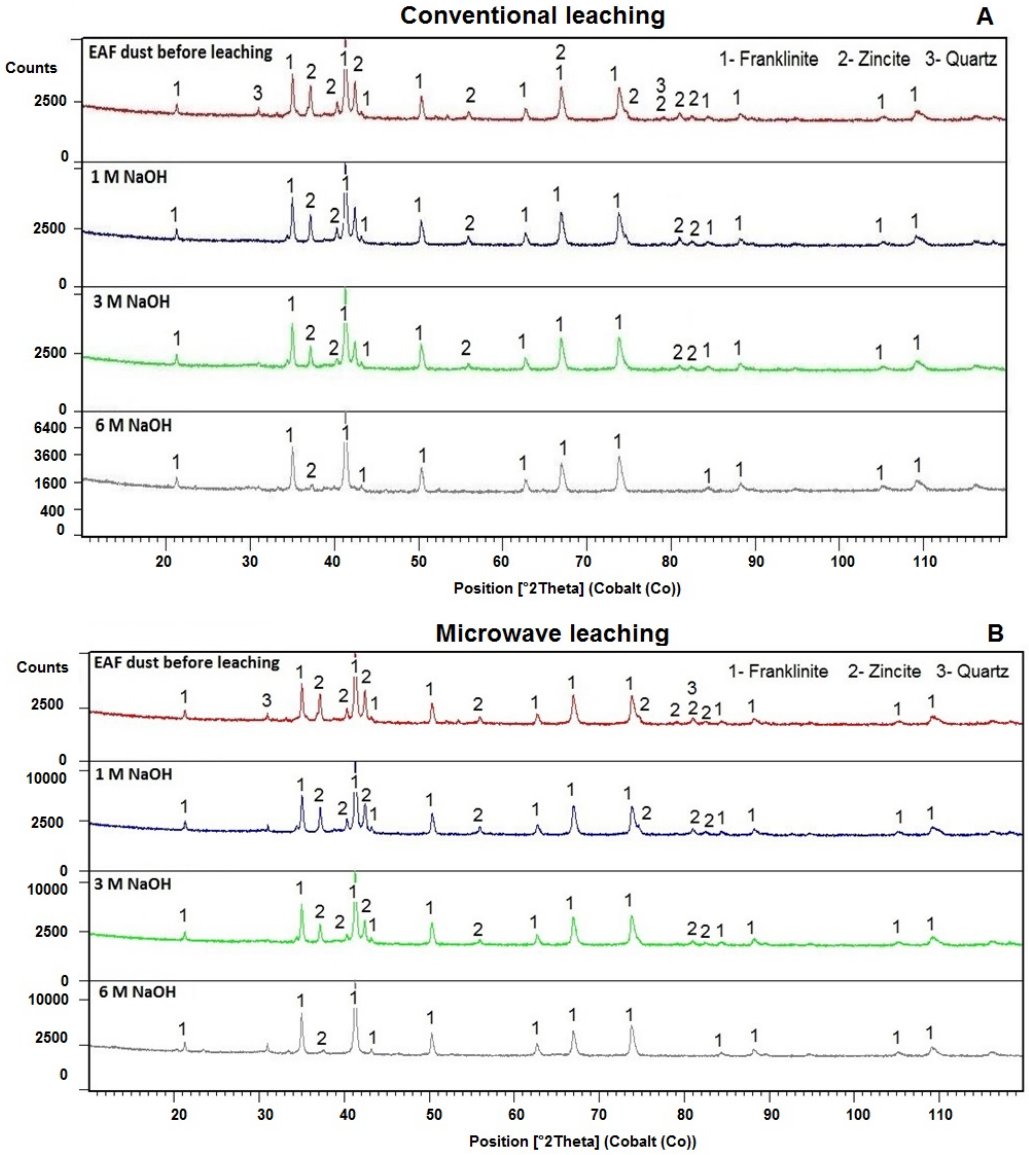

Fig. 9. Comparison of XRD patterns of different leaching residues after (A) conventional leaching and (B) MW-assisted leaching

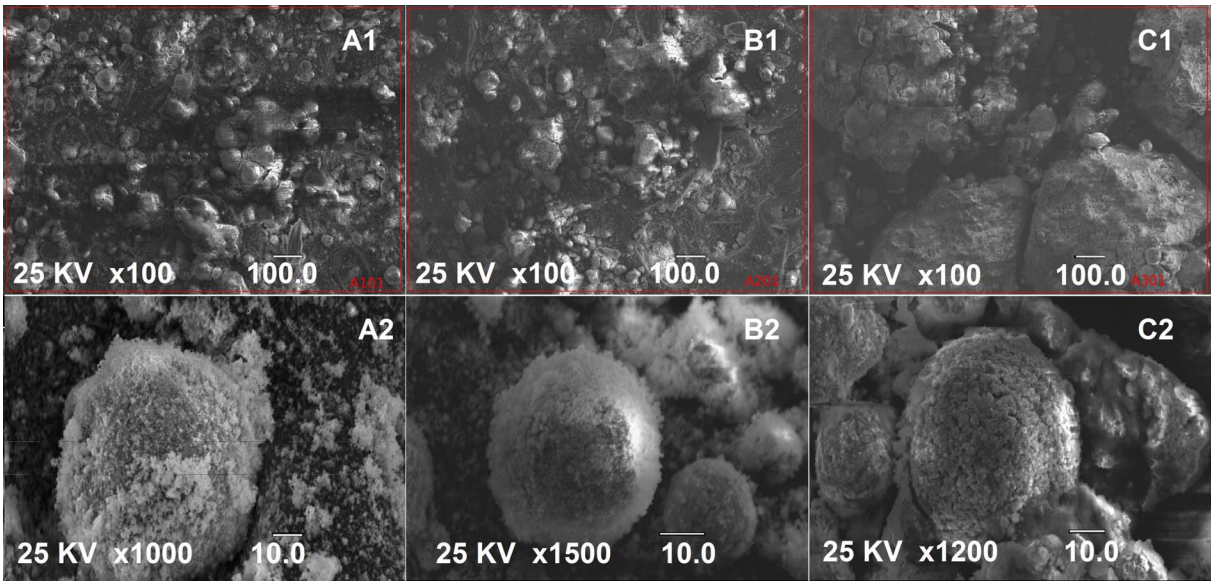

Fig. 10. SEM analysis of (A1, A2) the input EAFD sample and solid residues (B1, B2) after MW-assisted leaching and (C1, C2) after conventional leaching at various magnifications

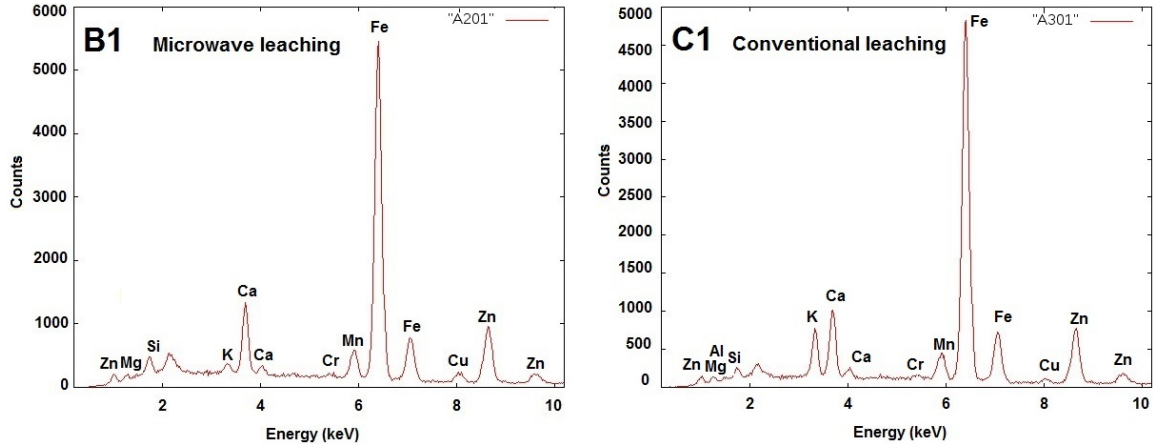

Fig. 11. EDS analysis of solid residue after MW-assisted leaching (B1) and conventional leaching (C1)

Acknowledgements

This work was supported by the Slovak Research and Development Agency under contract [APVV-14-0591]; and the Ministry for Education of the Slovak Republic under VEGA grant [1/0442/17]; and Research and Development Center of Zeleziarne Podbrezova, s.r.o. in framework of project LSPO. This article has been checked for spelling and grammar by Andrew J. Billingham.

REFERENCES

[1] https://www.worldsteel.org/media-centre/press-releases/2018/World-crude-steel-output increases-by-5.3--in-2017.html, accessed 09.10.2018

[2] T. Havlik, F. Kukurugya, D. Orac, L. Parilak, World Metall. – ERZMETALL. **65** (1), 48-56 (2012).

[3] http://www.nwcpo.ie/forms/EWC_code_book.pdf., accessed 09.11.2018.

[4] F. Kukurugya, T. Vindt, T. Havlík, Hydrometallurgy **154**, 20-32 (2015).

[5] G. Maruskinova, L. Parilak, V. Chomič, S. Turna, L. Brizekova, J. Havran, M. Roncak, in: Mater. recyklacia Priem. Odpad. Tale 53-59 (2018).

[6] Z. Sedlakova, T. Havlik, Acta Metall. Slovaca **12**, 209-218 (2006).

[7] M.H. Morcali, O. Yucel, A. Aydin, J. Min. Metall. Sect. B Metall. **48**, 173-184 (2012).

[8] Z. Sedlakova, H. Jalkanen, in: Espoo, Finland 41 (2005).

[9] Z. Hoang-Trung, F. Kukurugya, Z. Takacova, D. Orac, M. Laubertova, A. Miskufova, T. Havlik, J. Hazard. Mater. **192** (3), 1100-1107 (2011).

[10] M. Ranitovic, Z. Kamberovic, M. Korac, M. Gavrilovski, H. Issa, Z. Andic, Sci. Sinter **46** (1), 83-93 (2014).

[11] T. Havlik, G. Maruskinova, A. Miskufova, Arch Metall Mater **63** (2), 653-658 (2018).

[12] Z. Sedlakova, D. Orac, T. Havlik, Acta Metall. Slovaca. **12** (1), 338-345 (2006).

[13] F. Carranza, R. Romero, A. Mazuelos, N. Iglesias, J. Environ. Manage. **165**, 175-183 (2016).

[14] A.J.B. Dutra, P.R.P. Paiva, L.M. Tavares, Miner. Eng. **19** (5), (2006).

[15] M. Al-Harahsheh, S.W. Kingman, L. Al-Makhadmah, I.E. Hamilton, J. Hazard. Mater. **274**, 87-97 (2014).

[16] J. Veres, M. Lovas, S. Jakabsky, V. Sepelak, S. Hredzak, Hydrometallurgy **129-130**, 67-73 (2012).

[17] I. Mikhailov, S. Komarov, V. Levina, A. Gusev, J.P. Issi, D. Kuznetzov, J. Hazard. Mater. **321**, 557-565 (2017).

[18] M. Laubertova, T. Havlik, B. Hluchanova, in: Mod. trends Process. Second. raw Mater. non-ferrous Met. Kosice 67-71 (2008).

[19] M. Al-Harahsheh, S.W. Kingman, Hydrometallurgy **73** (3-4), 189-203 (2004).

[20] M. Al-Harahsheh, S.W. Kingman, C. Somerfield, F. Ababneh, Anal. Chim. Acta **638**, 101-105 (2009).

[21] I. Znamenackova, M. Lovas, S. Hredzak, S. Dolinska, in: SGEM Albena 965-973 (2014).

[22] X. Sun, J.-Y. Hwang, X. Huang, JOM **60** (10), 35-39 (2008).

[23] T. Havlik, M. Popovicova, M. Ukasik, Metall **56** (3), 131-134 (2002).

[24] E. Krakovska, H.M. Kuss, Rozklady v analytickej chemii. Kosice (2001).

[25] M. Al-Harahsheh, S.W. Kingman, I. Hamilton, J. Anal. Appl. Pyrol. **128**, 168-175 (2017).

[26] C.W. Bale, E. Belisle, P. Chartrand et al., Calphad. Comput. Coupling Phase Diagrams Thermochem. **54**, 35-53 (2016).

[27] D.K. Xia, C.A. Pickles, Miner. Eng. **13** (1), 79-94 (2000).

[28] S. Langova, D. Matysek, Hydrometallurgy **101**, 171-173 (2010).

[29] G. Orhan, Hydrometallurgy **78**, 236-245 (2005).

[30] P.E. Tsakiridis, P. Oustadakis, A. Katsiapi, S. Agatzini-Leonardou, J. Hazard. Mater. **179**, 1-3 (2010).

[31] I. Kobialkova, T. Havlik, WASTE – Second. Raw Mater. **5**, 4-7 (2013).

[32] A. Stefanova, J. Aromaa, O.A. Forsen, Physicochem. Probl. Miner. Process. **46**, 37-46 (2013).